Cyclotron-resonance study of polarons in GaAs-$Al_xGa_{1-x}As$ heterostructures

W. Seidenbusch
Institut für Experimentalphysik, Universität Innsbruck, A-6020 Innsbruck, Austria
(Received 29 January 1987)

Cyclotron-resonance transmission and emission experiments were performed in the two-dimensional electron system of an $Al_xGa_{1-x}As$-GaAs heterojunction using a nonresonant three-level excitation technique. It is found that in comparison to bulk GaAs, the polaron effect is reduced in the investigated energy range. The reduction of the polaron effect in the two-dimensional electron gas can be explained by occupation number effects. In addition, we determined the polaron effect in a hot-electron situation. At low electric fields the mass increase with energy is caused mainly by nonparabolicity. At electron temperatures above 100 K the polaron contribution to the effective mass reaches values observed in high-purity bulk GaAs.

I. INTRODUCTION

In bulk GaAs Lindemann *et al.*[1] determined from cyclotron-resonance (CR) spectra the contribution of the polaron effect of the effective mass and separated it from the band nonparabolicity. The interaction of the electrons with the LO phonons—the polaron effect—has been treated theoretically[2–7] and detected experimentally[8–12] in several quasi-two-dimensional (2D) systems. Das Sarma[3] has predicted an enhancement of the polaron effect for the 2D electron gas (2DEG) as compared to the three-dimensional (3D) case. Horst *et al.*[8] studied the electron-phonon interaction in an InSb space-charge layer and found an increased polaron interaction in the reststrahlen region. In contrast, Seidenbusch *et al.*[13] found in $Al_xGa_{1-x}As$-GaAs heterostructures a strong reduction of the polaron effect in a nonresonant situation. This reduction was explained qualitatively by occupation and screening effects. Also, Sigg *et al.*[11] found a strong suppression of polaron effects at low magnetic fields far off resonance. This paper presents a detailed study of the "polaron problem" by varying occupation and screening effects, on the one hand, by increasing the electron concentration, or, on the other hand, by heating up the electrons.

The details of samples and measurement technique are summarized in Sec. II. The calculation of the effective band-edge mass $m_0^*(2D)$ including band nonparabolicity (five-level $\mathbf{k}\cdot\mathbf{p}$ theory), polaron effects (perturbation theory), and occupation number effects is presented in Sec. III.

In Sec. IV we analyze quantitatively the CR spectra and we show that in the hot-electron regime the reduction of the polaron effect due to Landau-level filling is lifted by redistributing the carriers.

II. EXPERIMENTAL DETAILS

CR experiments were performed at far-infrared (FIR) frequencies in emission and absorption. A nonresonant three-level excitation technique is used where transitions between higher Landau levels (LL's) are induced by increasing the electron concentration or by carrier heating through an electric field. This technique has the advantage that the transmission can be measured even in the reststrahlen region, since the used radiation energy is essentially smaller than the phonon energy. A detailed description of the experimental technique can be found in Ref. 1. The transmission CR experiment can be performed in two different ways: The energy of the radiation can be tuned using a fixed magnetic field or the magnetic field can be varied at a constant radiation energy. The first way corresponds to an experiment with a Fourier transform spectrometer, the second with a FIR laser system. From the energy difference at a fixed magnetic field or from the magnetic field shift at a given energy of different LL transitions the amount of nonparabolicity and the polaron contribution to the effective electron mass are determined. CR transmission spectra were taken with the help of a FIR molecular laser which was pumped optically by a CO_2 laser. The FIR wavelengths were in the range of 50–200 μm. The samples were mounted in Faraday geometry and immersed in liquid helium in the bore of a magnet system. The FIR laser radiation was guided into the cryostat by an oversized light pipe and coupled to the sample with a cone. Depending on the wavelength range, a Ga-doped Ge detector or an extrinsic GaAs detector were used. The observed transition energy as a function of the magnetic field deduced from Fourier spectrometer and laser experiments is shown for sample 1 in Fig. 1. The zero-order transition energy $\hbar\omega_c^0 = \hbar eB/m_0^*$, which corresponds to the parabolic band structure (with $m_0^* = 0.065 m_0$), is represented by the dashed straight line. Since the deviation of the data points from the straight line is not increasing linearly with the magnetic field, this departure is due to nonparabolic effects like band nonparabolicity and polaron effect. The GaAs-$Al_xGa_{1-x}As$ heterostructures were grown by molecular-beam epitaxy (MBE). The mobilities and densities at 4.2 K are listed in the Table I.

CR emission experiments[14] were performed with the same samples. The emitted signal is measured with a narrow-band GaAs detector for a given frequency as a function of magnetic field. Since the linewidth of the

TABLE I. Properties of the investigated samples. The mobility and concentration were measured without illumination at 4.2 K.

	Al concentration (%)	Spacer thickness (Å)	Mobility ($cm^2/V\,s$)	Carrier density (cm^{-2})
1	35	370	4.00×10^5	1.2×10^{11}
3	35	360	1.00×10^6	2.0×10^{11}
4	40	220	6.10×10^5	2.3×10^{11}
5	33	240	6.00×10^5	2.4×10^{11}
6	33	100	2.20×10^5	2.5×10^{11}
7	32	60	3.10×10^5	4.1×10^{11}
8	37	50	1.64×10^5	2.9×10^{11}
9	28	120	4.36×10^5	2.9×10^{11}
10	36	190	7.50×10^5	3.3×10^{11}

GaAs detector is very narrow (0.25 cm^{-1}), this experiment is equivalent to a laser transmission experiment.

In the 2DEG the number of states per LL is given by the magnetic field. Therefore the Fermi level shows an oscillatory behavior for a given concentration with varying field. The position of the Fermi level is characterized by a dimensionless parameter, the filling factor ν, which is defined as the number of electrons divided by the number of states within one LL. Neglecting the spin, the filling factor can be expressed by $l^2\pi n_s$ with l the cyclotron radius and n_s the 2D density.

If ν is smaller than 1 only CR transitions 0-1 are possible, for ν close to 2 only transitions 1-2. The observable transitions are therefore unambiguously determined by the value of the filling factor. By illumination of the heterostructure with pulses from a light-emitting diode (LED) the 2D electron concentration and thus the filling factor is increased and different LL transitions are induced. The carrier concentration can be varied in different steps according to the pulse length of the band-gap radiation up to a factor of approximately 2 and is determined by Shubnikov–de Haas (SdH) oscillations.

The change of the carrier concentration by LED illumination causes a change in the band structure. This "light effect" is described in a previous paper[13] and has to be taken into account. The second way for inducing transitions between higher LL's in the transmission experiment is to heat up the samples by electric fields. We have used samples with Hall geometry as well as with Corbino geometry. It turned out that the laser transmission results were more consistent with the Corbino disc samples; in the emission experiments the geometry was not that critical.

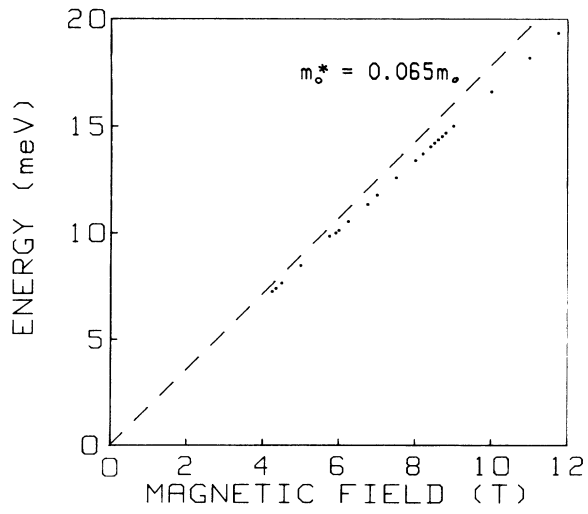

FIG. 1. Observed CR transition energy as a function of magnetic field in 2D AlGaAs-GaAs heterojunctions. The zero-order transition energy $\hbar\omega_c^0=\hbar(eB/m_0^*)$ is represented by the straight line.

III. THEORETICAL CONSIDERATIONS

In 3D-polaron experiments it has been demonstrated[1] that nonparapolicity is usually as strong as polaron effects. Therefore any polaron analysis must be based on a reliable $\mathbf{k}\cdot\mathbf{p}$ theory, which yields the bare energy levels. A simple analytical two-level approximation for polarons in the nonresonant regime has recently been derived by Das Sarma and Mason.[7] For a quantitative analysis it is necessary to insert the correct nonparabolic energy levels $E_n^0(\mathrm{NP})$ in the polaron calculation. For heterostructures Lassnig developed a self-consistent $\mathbf{k}\cdot\mathbf{p}$ theory,[15] a five-level scheme, which includes the penetration into the barrier material and many-body effects.

A. Nonparabolicity: $\mathbf{k}\cdot\mathbf{p}$ theory for 2D systems

The electronic wave function $\psi(k)$ is expanded in the vicinity of $k=0$ in terms of the symmetric Bloch functions $u_l(0)$:

$$\psi(k)=\sum_l f_l(k)u_l(0)\ ,$$

where the symmetric functions $u_l(0)$ oscillate rapidly, whereas the $f_l(k)$ are slowly varying envelope functions and describe the band mixing away from the band edge.

Diagonalizing the $\mathbf{k}\cdot\mathbf{p}$ matrix for the 2D system, the envelope function can be taken to be of the same form as in the three dimensions,

$$f=e^{ik_z z}\{\phi_1 \mid n\rangle,\phi_3 \mid n-1\rangle,\phi_5 \mid n+1\rangle,\phi_7 \mid n-1\rangle ,$$
$$\phi_2 \mid n+1\rangle,\phi_4 \mid n+2\rangle,\phi_6 \mid n\rangle,\phi_8 \mid n\rangle\} .$$

The plane wave $e^{ik_z z}$ and the constants ϕ_l are replaced in two dimensions by z-dependent envelope functions $\phi_l(z)$.

The following Schrödinger equation is obtained:

$$\left[U_c(z)+\frac{(n+\frac{1}{2})\hbar\omega_c}{\mu(\epsilon,z)}+\alpha(\epsilon,z)(\hbar\omega_c)^2 + \hat{P}_z\frac{1}{2m_0\mu(\epsilon,z)}\hat{P}_z\pm\frac{\lambda}{2}g^*(\epsilon,z)-\epsilon\right]\phi(z)=0 .$$

This equation describes the motion of two-dimensional electrons, which are quantized by the conduction-band potential $U_c(z)$. In the kinetic term as well as in the spin-splitting term the z-dependent quantities $\mu(\epsilon,z)$ and $g^*(\epsilon,z)$ appear, whose z dependence is caused by the local variation of the band edges. $\hbar\omega_c$ is the cyclotron-resonances energy of the free electron. For the heterostructure the potentials $U(z)$ have to be specified.

Figure 2 shows the local band structure for a GaAs-$Al_xGa_{1-x}As$ heterostructure. The band discontinuities are denoted as δ_c, δ_v, etc. and the resulting band-edge potentials for the effective Schrödinger equation are

$$U_c(z)=V(z)+\delta_c(-z) ,$$
$$U_v(z)=V(z)-E_0-\delta_v h(-z) ,$$
$$U_\Delta(z)=V(z)-E_0-\Delta_0-\delta_\Delta h(-z) ,$$
$$U_c'(z)=V(z)+E_1+\delta_c' h(-z) ,$$

where

$$U_\Delta'(z)=V(z)+E_1+\Delta_1+\delta_\Delta' h(-z) .$$

$h(z)$ is a continuous function which is necessary for the description of the "mixed" Bloch functions in the unit cells at the interface of the heterostructure.

$V(z)$ denotes the slowly varying space-charge potential which is the sum of the depletion and the Hartree potential

$$V(z)=\frac{4\pi e^2 N_d z}{\kappa_s}+4\pi e^2 N_{\rm el}\left[z-\int_{-\infty}^{z}dz'\rho(z')(z-z')\right]\Big/\kappa_s .$$

κ_s represents the static dielectric constant, N_d and $N_{\rm el}$ the depletion and inversion charge densities, $\rho(z)$ the normalized local carrier density.

The potentials have to be introduced into the effective Schrödinger equation in order to get the electronic energy levels. Through the electronic charge density in the Hartree potential the problem has to be solved self-consistently.

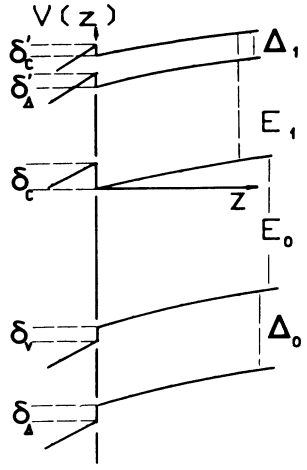

FIG. 2. Band-edge potentials for a GaAs-AlGaAs heterostructure, indicating the five-level approximation.

For the analysis and interpretation of our experimental data it is very important to know the contribution of nonparabolicity as exact as possible. Therefore the bare band structure, which can be calculated by the $\mathbf{k}\cdot\mathbf{p}$ theory self-consistently including the effects of exchange and correlation, must be known very precisely. A similar calculation by Stern and Das Sarma[16] is improved by using the correct expression in the kinetic energy according to the effective Schrödinger equation.

The depletion charge and the inversion charge are the main parameters of the calculation for the 2D system. Table II shows the relevant band-edge parameters which

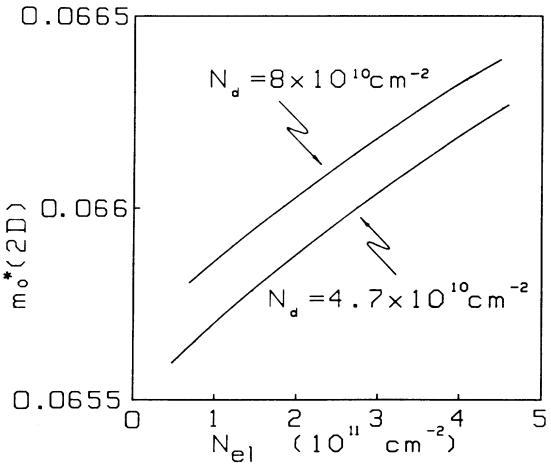

FIG. 3. Effective 2D band-edge mass $m_0^*(2D)$ for a GaAs-$Al_{0.3}Ga_{0.7}As$ heterostructure as a function of the electron concentration for two depletion concentrations.

TABLE II. Band-edge parameters E_0, E_1, Δ_0, Δ_1 (all in eV), effective mass m_0^* (in units of m_0), and effective g factor g_0^* for GaAs and $Al_{0.3}Ga_{0.7}As$.

	E_0	E_1	Δ_0	Δ_1	m_0^*	g_0^*
GaAs	1.519	3.140	0.341	−0.171	0.065	−0.44
$Al_{0.3}Ga_{0.7}As$	1.900	2.842	0.310	−0.171	0.086	0.45

are used. For the band offset $\delta_c = 0.7(E_{0\,Al_xGa_{1-x}As} - E_{0\,GaAs})$.

Now the 2D band structure can be expressed in terms of an effective 2D mass $m_0^*(2D)$ and an effective 2D band gap $E_m^*(2D)$. Neglecting spin splitting, we can write

$$E_{n+1} - E_n = \hbar\omega_c / m_2^*(n) ,$$

$$m_2^*(n) = m_0^*(2D) + 2n\hbar\omega_c / E_m^*(2D) .$$

$m_0^*(2D)$ and $E_m^*(2D)$ depend on N_d and N_{el}, whereas $m_0^*(2D)$ is influenced mainly of the kinetic energy in the z direction, and $E_m^*(2D)$ includes the influence of motion parallel to the interface. Figure 3 shows the dependency of $m_0^*(2D)$ on the inversion charge N_{el} and the depletion charge density N_d. The increase of the "effective" band-edge mass is about 1% in the given density range. The effective gap $E_m^*(2D)$ is changed only weakly by the two dimensionality, giving a value of 1.405 eV.

B. Magneto-polarons in the 2DEG

The Fröhlich interaction in the 2DEG is considerably stronger than in three dimensions due to the concentration of the wave function in the 2DEG.[3–5] In a real 2D system, where the wave function is spread out over several 100 Å, the effective interaction is reduced and can be expressed by means of a form factor $F(q)$,

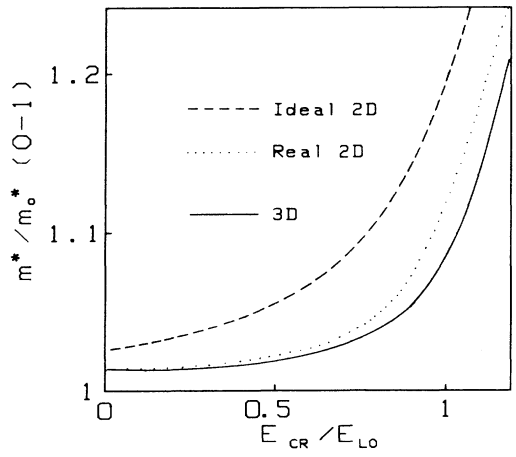

FIG. 4. Comparison of the polaron mass shift for the 0-1 transition for the indicated systems.

$$V_{eff}(q) = \frac{e^2\hbar\omega_L}{4q}\left[\frac{1}{\epsilon_\infty} - \frac{1}{\epsilon_0}\right]F(q) .$$

$F(q)$ includes the influence of the z-dependent part of the electron wave function and is equal to 1 for the ideal case (δ function in the z direction). For the Stern-Howard wave function, $F(q)$ is given by[6]

$$F(q) = \left[1 + \frac{9q}{8b} + \frac{3q^2}{8b^2}\right] \Big/ \left[1 + \frac{q}{b}\right]^3 .$$

When we start the perturbation series from the bare energy levels E_n^0, the polaron shift in the single-particle approximation is given by

$$\delta E_n = \sum_{m,q} M_{nm}^2(q) V_{eff}(q) / (E_n^0 - \delta E_n - E_m^0 - \hbar\omega_L - \delta E_0) .$$

$M_{nm}(q)$ denote the matrix elements between Landau levels (n,m). Figure 4 shows a quantitative comparison of the strength of the polaron effect for a parabolic band.

C. Occupation number effects

Due do the Pauli's exclusion principle, which does not allow the interaction with an occupied state, the effective polaron interaction with a partially occupied Landua level (with a filling factor ν) has to be reduced by a factor $1-\nu$. This means that in a lowest-order many-body approximation this reduction has to be taken into account.

The presented theoretical considerations are valid in the regime of the resonant polaron interaction, which is demonstrated by Lassnig,[17] who describes well the experimental data taken in the magnetic field from 10 to 22 T. In the range of lower magnetic fields or higher filling factor values the nonresonant contribution of the polaron interaction gets more important. In this case the dynamic screening, which is not included in this theory, cannot be neglected anymore. It will be shown that an extrapolation of the theoretical curve can be accepted down to approximately 8 T.

IV. RESULTS

Figure 5 shows typical transmission spectra as a function of the magnetic field for the laser wavelength of 96 μm. Before the illumination the electron concentration is 2.4×10^{-11} cm^{-2} ($\nu = 0.66$). With increasing filling factor (>1) a shift of the resonance position to higher magnetic fields is observed. This shift is the result of the superposition of different transitions (0-1, 1-2).

If the filling factor is smaller than 1 only the transition between the LL 0-1 can be observed. Calculating the probabilities for different transitions, it turns out that in

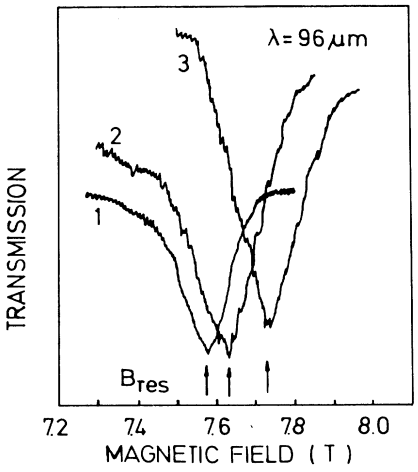

FIG. 5. CR transmission spectra at a wavelength of 96 μm for different values of filling factor: 1, $\nu=0.66$, $B_{res}=7.57$ T, linewidth equals 1.9 cm^{-1}, transition 0-1; 2, $\nu=1.30$, $B_{res}=7.63$ T, linewidth equals 2.49 cm^{-1}, transition 0-1 and 1-2; 3, $\nu=1.62$, $B_{res}=7.73$ T, linewidth equals 2.77 cm^{-1}, transition 1-2.

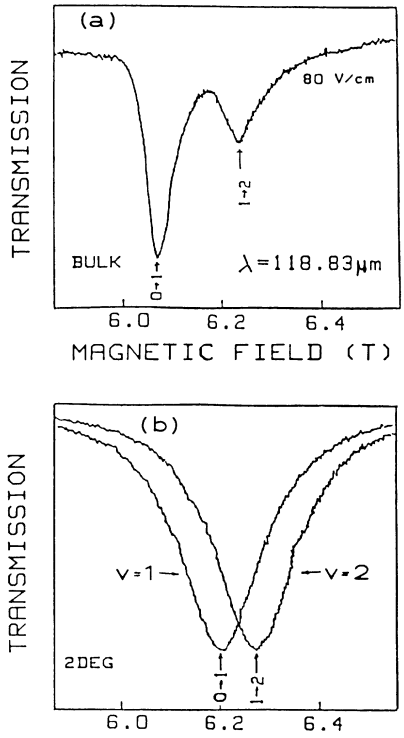

FIG. 7. CR transmission spectra for (a) a bulk GaAs sample and (b) heterostructure. Two lines are observed in the bulk case due to electric field heating. In the 2D case single lines for different ν (different electron concentration) are shown.

the range of the filling factor from 1 to 1.6 a superposition of the two transitions 0-1 and 1-2 must be observable, whereas in the range from 1.6 to 2 only the 1-2 LL transition occurs. This can be well demonstrated by observing the measured CR mass as a function of the filling factor for sample 6 in Fig. 6. This means that it is important to take the value of the shift in the range of the filling factor where no superposition of two transitions exists.

Figure 7 shows a comparison of a bulk CR spectrum (obtained for high-purity GaAs) with a spectrum obtained for a heterostructure. Two CR transitions are seen (0-1, 1-2). In the bulk case the higher transition is induced by the given electric field. In the 2D case the population of $n=1$ is achieved by light illumination. It is obvious that the splitting between the lines is considerably smaller for the 2D case. Figure 8 shows the dependency of the line splitting on the CR energy for the bulk case and the 2DEG. The splitting for the 2D case is considerably smaller in the whole range. The curves represent theoreti-

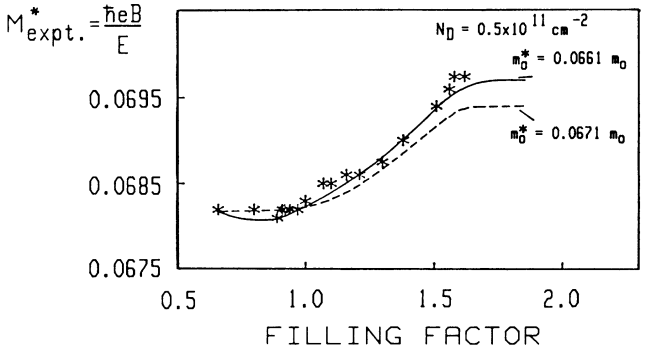

FIG. 6. Dependence of the cyclotron mass on the filling factor. The continuous increase between 1 and 1.6 is due to the superposition of the transitions 0-1 and 1-2. Dashed curve: theoretical curve using the nonparabolicity model. Solid curve: in addition the changed band structure is included.

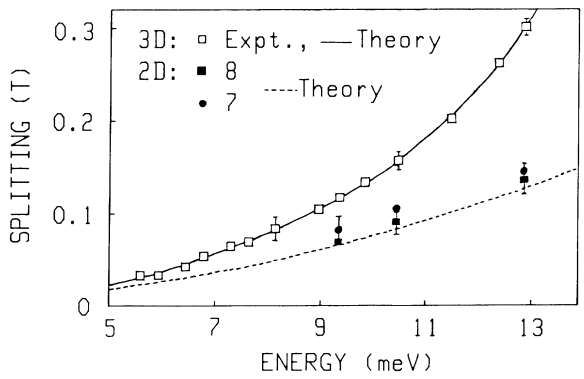

FIG. 8. Observed Landau transition energy difference (corresponding to the splitting of the lines in Fig. 7) plotted as a function of laser energy. The solid curve is a theoretical fit including nonparabolicity and polaron effects. The dashed curve includes only nonparabolicity.

cal calculations of the splitting[1] in the 3D case including polaron effects and nonparabolicity (solid curve) and only nonparabolity (dashed curve) for the 2D case. It is evident that in the 2DEG the splitting is caused mainly by the nonparabolicity.

Lassnig demonstrated[17] that a consistent polaron analysis including wave-function effects, nonparabolicity, and nonresonant contributions can well describe experimental data within lowest-order many-body approximation. Traditional screening calculations, especially static screening, are not useful because they lead to unphysical results. This means that the experimental data can be explained only with occupation number effects in the high magnetic field region.

A comparison of the experimental CR masses for the 0-1 and 1-2 transitions for the 3D and the 2D cases is shown in Fig. 9. For the bulk material the experimental data agree very well with the theoretical calculations including $\mathbf{k}\cdot\mathbf{p}$ theory for the nonparabolicity and an improved Wigner-Brillouin perturbation theory for the polaron effect taking a band-edge value of 0.065 for the effective mass and 0.083 for the Fröhlich parameter.

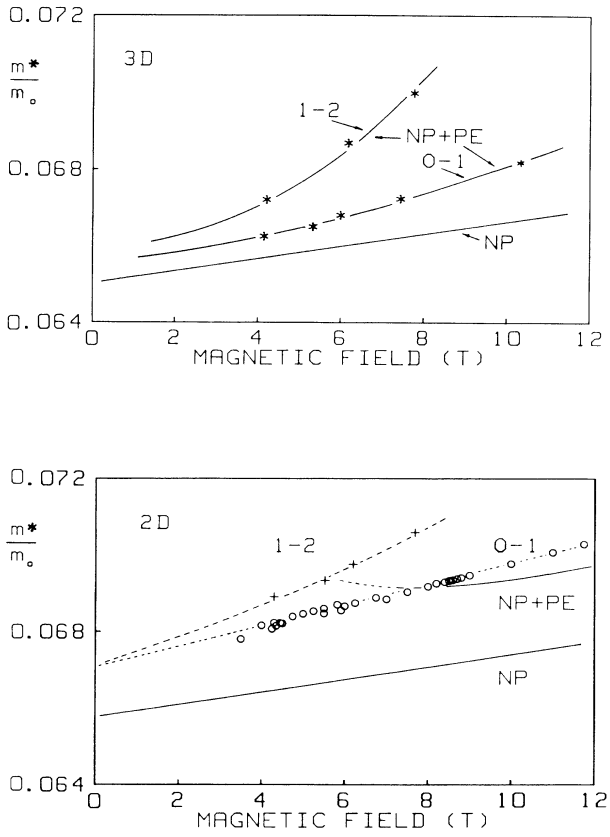

FIG. 9. Comparison of the dependence of the effective mass of the 3D and 2D systems for the 0-1 and 1-2 transitions. The solid curves are the result of calculations including nonparabolicity (NP) respectively nonparabolicity and the polaron effect (NP + PE). The dashed curves are for guiding the eye.

If we now concentrate the discussion to the 2D case we see that the band-edge value of the mass at zero field is higher but the increasing of the CR mass is weaker. The band-edge mass is changed due to the fact that a higher carrier concentration and higher depletion potential create a higher nonparabolicity (see Fig. 3). Since the slope of the nonparabolicity contribution is slightly smaller than the slope of the experimental data, a small contribution of a resonant polaron effect can be deduced. Especially the different increasing behavior of the 3D and 2D curves for the 1-2 transition is a sign for the strong reduction of the polaron effect in the 2D case. It is evident from the plot that the presented theory is applicable down to 8 T. For the lower magnetic field range there is no theory available, which should take into account dynamic screening effects.

A. Temperature-dependent screening of polaron interactions

1. CR emission

The CR emission signal is measured with a narrow-band GaAs detector for a given frequency as a function of magnetic field for different applied electric fields. Since the linewidth of the detector is 0.25 cm^{-1}, this experiment is equivalent to a laser transmission experiment. A comparison of the CR emission spectra for a bulk GaAs sample and a heterostructure sample for two electric fields and a CR energy of 9.25 meV is shown in Fig. 10. The spectra consist of two lines due to 1-0 and 2-1 transitions. It can be seen clearly that the splitting between the lines is small for the heterostructure at the lower field, but it gets comparable to the bulk value for the higher electric field.

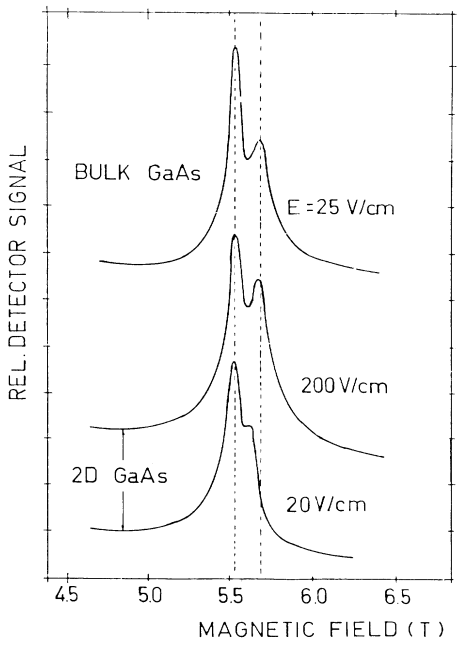

FIG. 10. CR emission spectra as detected with a narrow-band detector at 9.25 meV as a function of emission magnetic field for different electric fields.

2. CR transmission

From the analysis of CR transmission spectra for several laser frequencies as a function of electric field, information about carrier heating and screening of polaron interactions can be obtained. In previous experiments[13] using samples with carrier concentrations larger than 3.0×10^{11} cm^{-2} only a broadening of the transition line but no line splitting due to different transitions was observable.

In more recent experiments we have investigated samples with carrier concentrations below 2×10^{11} cm^{-2}. With these samples clear evidence for higher Landau transitions is found. At low electric fields the spectrum consists of one single line which starts splitting with increasing electric field until a double line structure is clearly resolved at the higher field value. Figure 11 shows the splitting as a function of electric field. The splitting between the observed transitions which corresponds to the energy differences between the two lowest Landau transitions starts at a given value and increases for fields higher than 20 V/cm and reaches a saturation value at the highest field. Also, data from emission experiments for two different emission energies selected by a narrow-band GaAs detector are shown. Both experiments yield a good agreement showing an electric-field-dependent mass change for different LL transitions. Analyzing the data theoretically, it turns out that for low electric fields the splitting corresponds to the bare nonparabolicity, and that it increases at the highest field to the value observed in the bulk. Through the electron heating an additional contribution to the mass change with energy is found. Since the nonparabolicity is not electric field dependent in the used field range, this contribution can only result from an increased contribution due to the electron–polar-optical-phonon interaction. This is the first direct confirmation of an electron temperature and thus population-dependent polaron effect.

In addition, by analyzing the spectra with respect to the peak intensities, one gets the value of the electron temperature[12]

$$T_{n,n-1}=\frac{\hbar\omega_c}{k_B}\left[\ln\frac{(n+1)I_{n-1,n}}{nI_{n,n+1}}\right]^{-1}$$

when n denotes the number of the LL's and I the absorption intensities. The electron temperature rises slowly for electric fields up to 50 V/cm and reaches saturation values in the range of 100 K. In a very recent paper[18] it is shown that the mass which is associated with the transition between the lowest Landau levels increases with temperature for values up to 100 K. This is further evidence that at higher temperatures the screening and occupation number effects are reduced.

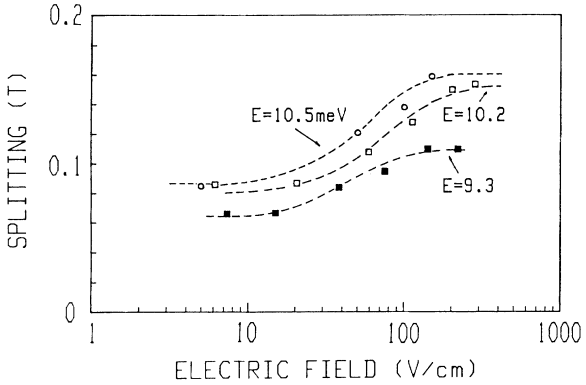

FIG. 11. Electric field dependence of the line splitting. The circles represent transmission data; the squares emission data. The transition energies are indicated.

V. SUMMARY

We present CR data of the 2DEG system of $Al_xGa_{1-x}As$-GaAs heterojunctions. For analyzing the Landau-level transitions a model is used that includes nonparabolicity of the conduction band and that evaluates polaron effects from an improved perturbation theory. In comparison to the splitting values of the bulk GaAs the values in the 2DEG are essentially smaller and can be described by the nonparabolicity and a reduced polaron contribution. This reduction is due to occupation number effects. In the hot-electron situation the polaron effect is restored due to the creation of empty places in the lowest Landau level with temperature. In addition, dynamic screening effects are reduced.

ACKNOWLEDGMENTS

This work is supported by the Stiftung Volkswagenwerk, Project No. I 61840 and by the Jubiläumsfonds der Österreichischen Nationalbank, Project No. 2907. I thank Professor E. Gornik and Dr. R. Lassnig for valuable discussions. The samples were provided by Dr. G. Weimann, Forschungsinsitut der Deutschen Bundespost, Darmstadt.

[1]G. Lindemann, R. Lassnig, W. Seidenbusch, and E. Gornik, Phys. Rev. B **28**, 4693 (1983).
[2]S. Das Sarma and A. Madhukar, Phys. Rev. B **22**, 2823 (1980).
[3]S. Das Sarma, Phys. Rev. B **27**, 2590 (1983).
[4]D. M. Larsen, Phys. Rev. B **30**, 4595 (1984).
[5]F. M. Peeters and J. T. Devreese, Phys. Rev. B **31**, 3689 (1985).
[6]R. Lassnig and W. Zawadzki, Surf. Sci. **142**, 388 (1984).
[7]S. Das Sarma and B. A. Mason, Phys. Rev. B **31**, 1177 (1985).
[8]M. Horst, U. Merkt, and J. P. Kotthaus, Phys. Rev. Lett. **50**, 754 (1983).
[9]E. Gornik, R. Lassnig, H. J. Störmer, W. Seidenbusch, A. C. Gossard, W. Wiegmann, and M. von Ortenberg, in *Proceedings of the 17th International Conference on the Physics of Semiconductors, San Francisco, 1984*, edited by D. J. Chadi and W. A. Harrison (Springer, Berlin, 1985), p. 303.
[10]M. Horst, U. Merkt, W. Zawadzki, J. C. Maan, and K. Ploog, Solid State Commun. **53**, 403 (1985).
[11]H. Sigg, P. Wyder, and J. A. A. J. Perenboom, Phys. Rev. B **31**, 5253 (1985).
[12]W. Seidenbusch, E. Gornik, and G. Weimann, Physica **134B**,

314 (1985).
[13]W. Seidenbusch, G. Lindemann, R. Lassnig, J. Edlinger, and E. Gornik, Surf. Sci. **142**, 375 (1984).
[14]E. Gornik, W. Seidenbusch, R. Lassnig, H. L. Störmer, A. C. Gossard, and W. Wiegmann, *Two-Dimensional Systems, Heterostructures, and Superlattices,* Vol. 53 of *Springer Series in Solid-State Sciences,* edited by G. Bauer, F. Kuchar, and H. Heinrich (Springer, Berlin, 1984), p. 60.
[15]R. Lassnig, Phys. Rev. B **31**, 8076 (1985).
[16]F. Stern and Das Sarma, Phys. Rev. B **30**, 840 (1984).
[17]R. Lassnig, Surf. Sci. **170**, 549 (1986).
[18]M. A. Brummel, R. J. Nicholas, and M. A. Hopkins, Phys. Rev. Lett. **58**, 77 (1987).